Synthesis and analysis of hexagonal ferrite for microwave absorption application in X-band

MONIKA RANI[1], KAMALJIT SINGH BHATIA[2], HARJITPAL SINGH[3], HARSIMRAT KAUR[3], NANCY GUPTA[4], SANDEEP RANA[2]
[1] *I.K Gujral Punjab Technical University, Jalandhar, Punjab, India*
[2] *G.B Pant Institute of Engineering and Technology, Pauri Garhwal, Uttrakhand, India*
3C.T. Institute of Engineering Management and Technology, Shahpur Jalandhar, Punjab, India
[4]*Layallpur Khalsa College of Engineering, Jalandhar, Punjab, India*

The synthesis of M-type $Ba_{0.5}Sr_{0.5}Co_xGa_xFe_{12-2x}O_{19}$ hexagonal ferrite has been performed using conventional ceramic method on which electromagnetic wave absorption in the frequency ranges from 8.2GHz to 12.4 GHz has been observed for the variable composition values. This help us to infer that the refection loss boosts -33.36 dB in the composition x=0.4 at 9.62 GHz at thickness of 2.0 mm. The variations were from -10dB to -20dB in the frequency range of 8.2GHz to 8.704 (B.W 0.5 GHz) & 9.96GHz to 10.97GHz (B.W 1.01GHz) and less than -20dB in the range of 8.78GHz to 9.88GHz (B.W 1.1GHz). Hence the synthesized magnetic ferrite can be used as a substrate for different antennas in X-Band because of the deduced insights in the paper.

(Received August 2, 2020; accepted August 10, 2022)

Keywords: Reflection loss, Doping, Energy dispersive spectra (EDAX), Absorption bandwidth

1. Introduction

In the present scenario, whole world is very much dependent on growing electromagnetic wave technologies like Wi-Fi, WIMAX, and Mobile communication, adhoc Network, RADAR and Satellite Communication. These large electromagnetic radiations in the atmosphere interfere with each other and create EMI effect. This EMI effect not only degrades the functioning of our electrical/electronic devices but can collapse them also. To counterpart this, the need of electromagnetic absorbing material (EAM) has fascinated a lot of researchers and M-type hexagonal ferrite was being identified as a best microwave absorbing material. To further increase the absorption capability of ferrites, process of doping has been adopted [1][2]. These ferrites are non-metallic materials having high resistivity, chemical stability and strong magnetic properties Since a few decades, various studies were being done on the substitutions of dopant in hexagonal ferrites to change their properties like permittivity, permeability, hysteresis, coercivity and absorption properties. Mosleh et al. synthesized a M-type $Ba_{1-x}Ce_xFe_{12}O_{19}$ hexagonal ferrite and found -16.43dB reflection loss in the X-band [3]. Baykala et al. had reported that microwave absorption got enhanced with the addition of Pb^{2+} in M-type Ba-Sr hexagonal ferrite [4]. Syazan et al. synthesized a Co-Ti and Mn-Ti substituted Barium Ferrite and observed a significant dip in reflection loss of -31.27dB and -26.73dB respectively [5]. Deng et al. had composed a M-type Barium hexaferrite with the nominal composition of $BaZr_xFe_{(12-x)}O_{19}$ (x=0.0,0.3,0.6, 0.9 & 1.2) and observed improvement in refelection loss with increasing x i.e. -30.3 dB at x=1.2 sample [6]. Gunanto et al. had synthesized M- type Ba-Sr hexagonal ferrite with varying composition of Si rubber and found varying RL with composition i.e. -15 dB for 20% composition at 10.8 GHz & decreasing onwards [7]. Araz et al. had reported -20dB RL with Co doping at frequency range 2-18 GHz [8]. Guo et al. had observed the variation of reflection loss with thickness of Co^{2+} doping material in Ba-Sr hexaferrite and recorded -43.6dB RL at 4.3mm and -45.8dB at 2.8mm thickness [9].

A lot of researches have been made earlier for increasing the absorption or attenuation in microwave frequency range. They have shown development in this field by increasing magnetic and dielectric losses and structural parameters. Rosdi et al. presented an absorption property of Mg-Ti doped M-type barium hexagonal ferrite. He observed improved reflection loss of -22.59 dB at 9.42 GHz with 3mm thickness of material and -10 dB bandwidth of 0.14 GHz. It was the matching between magnetic and dielectric loss that resulted in large microwave absorption. Mechanism of hysteresis was considered but it was not clearly mentioned how this parameter effect microwave absorption [10]. Feng et al. investigated the characteristics of Co doped M-type Barium hexagonal ferrite in the frequency range 2 GHz -18 GHz. He observed large return loss of 32.1 dB at 11.2 GHz in the frequency range 8.5 GHz-13.5 GHz with thickness of 2.00mm at x=0.4. Further, he concluded that large magnetic losses resulted in this much of return loss and there is no role of hysteresis and input impedance in microwave absorption [11] . Narang et al. gave Ba-La-Na doped M-type Co-Ti-Mn hexagonal ferrite and discussed the microwave absorption properties in between 18 GHz-26.5GHz. He observed large losses and impedance matching resulted in high return loss of -45.94

at 1.30mm thickness with -10 dB absorption bandwidth of 8.33 GHz [12]. Isa Araz had concluded that $Ba_{0.5}Ce_{0.5}Fe_{11}CoO_{19}$ hexagonal ferrite show microwave absorption properties in the range 2 GHz- 18 GHz. He mentioned the role of loss tangent for the observed absorption and return loss which was -31.4 dB at 11 GHz with 3mm thickness [13]. Khandani et al. formed a Ce-Nd doped Sr hexagonal ferrite that has given absorption properties in the X-band range. The observed RL was -8.7 dB at 2.5mm thickness which was resulted due to behaviour with magnetic loss tangent. The role of hysteresis parameters were discussed [14]. Liu et al. made a $BaFe_xTio_{19}$ ferrite and observed its microwave absorption characteristics at 26.5 GHz -40 GHz. He had varied the material ratio (Fe/Ba) to find the maximum microwave absorption rate. The highest value of RL i.e.-37.1 dB was observed at 35 GHz with 2.8mm of thickness [15]. Li et al. had prepared M-type Ba hexagonal ferrite with doping of Co-Zr in X-band frequency range. The conclusion of his experiment was that the absorption depends majorly on magnetic and dielectric losses. The results of his research demonstrate RL of -28.7 dB at 16.44 GHz with 1.6mm thickness [16]. Torabi et al. synthesized M-type Ba hexagonal ferrite doped with Mn-Co-Gd at frequency 2-18 GHz. The return loss was increased up to -48 dB at 17.2 GHz at 5.6mm thickness [17]. Mahadevan et al. synthesized two materials $BaFe_{12}O_{19}$ and $BaFe_{11.5}Ti_{0.5}O_{19}$ hexagonal ferrite and compared the microwave absorption properties of both at frequency range 12GHz-18GHz. Microwave absorption properties was found to be more superior in second composition [18].

From the literature survey presented above, it was concluded that a lower thickness ferrite material is best suited for better microwave absorption, high RL and large bandwidth. While taking into consideration the above results of literature, we have synthesized M-type $Ba_{0.5}Sr_{0.5}Fe_{12}o_{19}$ hexagonal ferrite using Ga^{3+} and Co^{2+} as dopant materials on the frequency range 8.2GHz - 12.4GHz at temperature 1100 degree Celsius for 15 hrs and we acquired the improved results.

2. Experimental procedure

We have used standard ceramic method to synthesize M-type $Ba_{0.5}Sr_{0.5}Co_xGa_xFe_{(12-2x)}$ O_{19} (x=0.0,0.2,0.4,0.6,0.8 and 1.0) hexagonal ferrite [19]. The chemicals used for synthesisation are $BaCo_3$ (Sigma-Aldrich 99.98%pure), $SrCo_3$ (Sigma-Aldrich 99.98%pure), $CoCo_3$ (Sigma-Aldrich 99.98%pure), Ga_2O_3 (Sigma-Aldrich 99.98%pure) & Fe_2O_3 (Sigma-Aldrich 99.98%pure). The process of synthesisation started with grinding of mixing of material in distilled water using electrically controlled pestle–mortar furnace for 8 hours. After that, mixture was dried at room temperature. The dried powder was pre-sintered at 1000°C for 10 hours in automatic electric furnace which was programmed to do the same. Again, powder was allowed to cool down and re-grinded for 8 hours. Granulation of powder was performed using sieving of mesh size 220B.S.S. Lastly, the fine powder was converted into pallets using hydraulic press at 75KN/m^2 pressure and this pallet was again sintered at 1100°C for 15 hours.

3. Results and discussion

XRD Analysis: At the time of the analysis, for the composition of x= 0.0 & 0.2 there was the only primary phase of the material, but for the composition value of x>0.2, there was secondary phase of $BaFe_2O_4$ the orthorhombic. The prepared sample of hexagonal ferrite $Ba_{0.5}Sr_{0.5}Co_xGa_xFe_{12-2x}O_{19}$ for composition of x = 0.0, 0.2, 0.4, 0.6, 0.8,1.0 are analysed in such a way their reaction can be observed to the applied force i.e., mechanical, with the help of the diffraction technique which includes X rays as shown in the Fig.1 and also the sample is analysed for their purity of the phase. Millar indices are used as the to calculate the diffraction patterns formed by the sample. According to the results there is formation of M-type hexagonal shaped phase, with no peaks in the other phases. In the JCPDS file no. 51-1879, a = 5.8862 Å, c = 23.137 Å and V = 694.24 $Å^3$, similar kind of M-type crystal structure is formed.

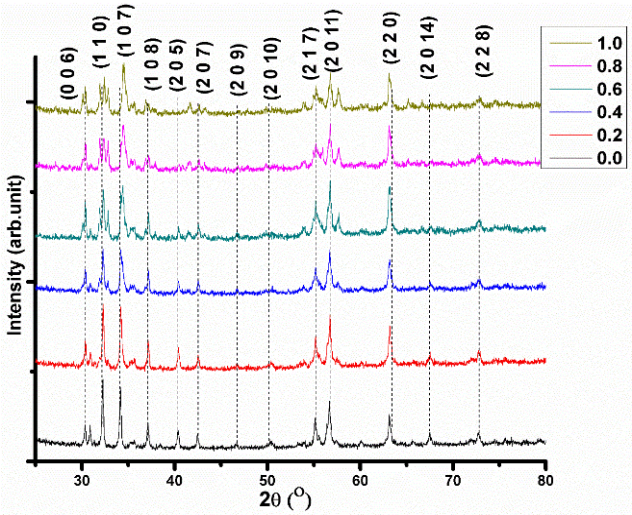

Fig. 1. X-ray diffraction method analysis of $Ba_{0.5}Sr_{0.5}Co_xGa_xFe_{12-2x}O_{19}$ (x = 0.0, 0.2, 0.4, 0.6, 0.8, 1.0) samples (color online)

In order to confirm the chemical composition of $Ba_{0.5}Sr_{0.5}Co_xGa_xFe_{12-2x}O_{19}$ hexagonal ferrites synthesized using a standard ceramic method and sintered at 1100 °C for 15 hours, the energy dispersive spectra (EDAX) of the typical compositions (x = 0.2, 0.4, 0.6, 0.8 and 1.0) were recorded at room temperature and obtained EDAX spectra are shown in Fig. 2. The EDAX spectra of all samples explain the presence of Ba, Sr, Fe, Co and Ga in all compositions.

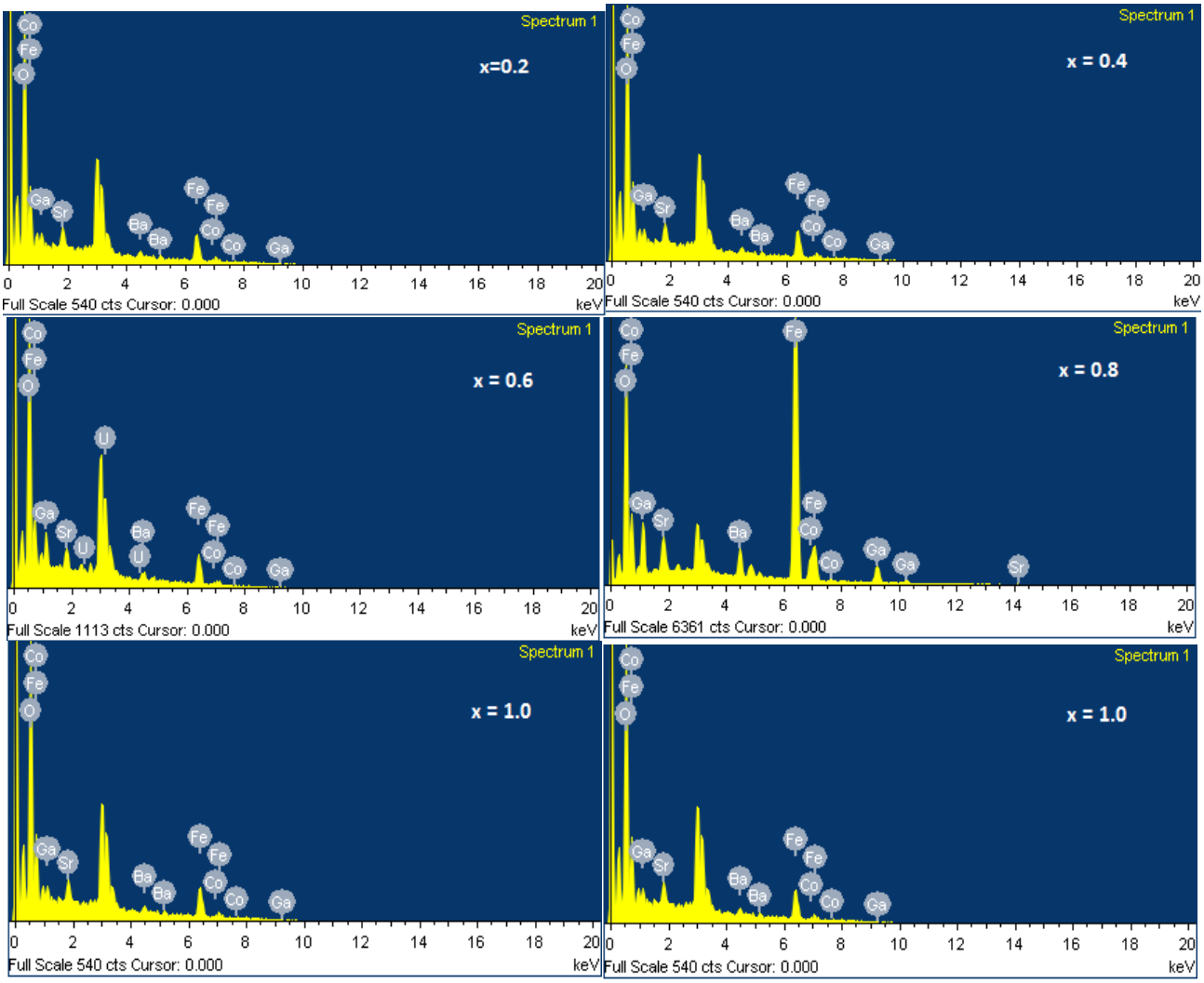

Fig. 2. Energy dispersive spectroscopy spectra of $Ba_{0.5}Sr_{0.5}Co_xGa_xFe_{12-2x}O_{19}$ (x = 0.2, 0.4, 0.6, 0.8 and 1.0) hexagonal ferrite compositions (color online)

The observed chemical composition data of same compositions is summarized in Table 1. It is observed that some other extra elements are also observed in the compositions of 0.4 and 0.6. The weight ratio and atomic weight ratios as observed from EDAX are also mentioned in Table 1.

The scanned electron micrographs of the undoped [x=0.0] and doped composition [x = 0.4, 0.6, 1.0] shows that the grain size was larger before the doping and afterwards its size decreases. The grains in the doped composition exhibits non-uniformity in the size and distribution. The SEM and mean crystalline size, shows the physical size and mean structural coherence length respectively.

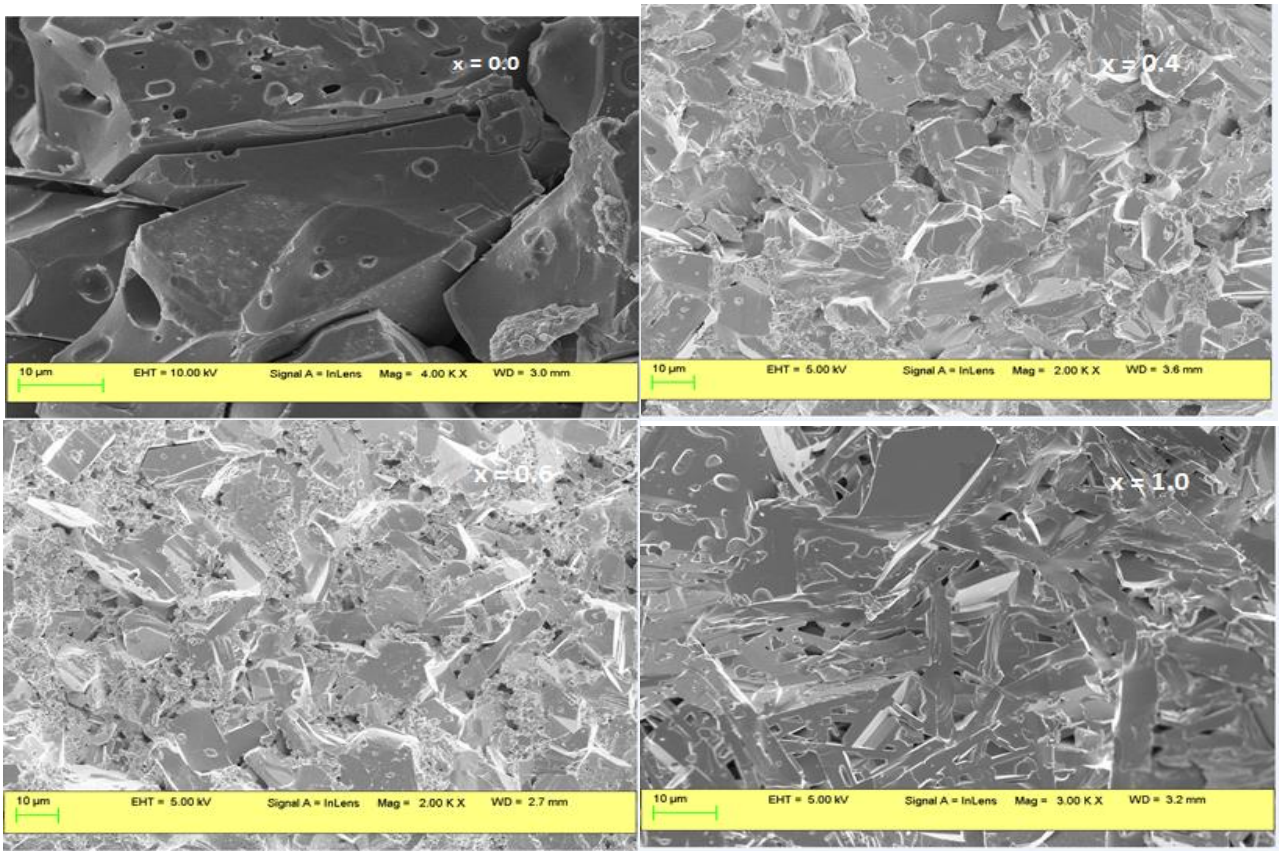

Fig. 3. Scanned electron micrographs of $Ba_{0.5}Sr_{0.5}Co_xGa_xFe_{12-2x}O_{19}$ (x = 0.0, 0.4, 0.6 and 1.0) hexagonal ferrite compositions prepared using standard ceramic method and sintered at 1100 °C for 15 hours (color online)

Table 1. Elemental composition weight & atomic percentage of typical samples of $Ba_{0.5}Sr_{0.5}Co_xGa_xFe_{12-2x}O_{19}$ (x = 0.2, 0.4, 0.6, 0.8 and 1.0) hexagonal ferrites

Element	Weight %	Atomic %	Weight %	Atomic %	Weight %	Atomic %	Weight %	Atomic %	Weight %	Atomic%
	0.2		0.4		0.6		0.8		1.0	
O	30.92	64.71	22.94	62.54	23.46	63.12	25.06	56.54	30.92	64.71
Fe	49.37	29.60	28.74	22.45	24.82	19.14	49.98	32.24	49.37	29.60
Co	-1.78	-1.01	5.14	3.80	7.72	5.64	4.12	2.52	-1.78	-1.01
Ga	3.35	1.61	2.71	1.70	4.68	2.89	10.15	5.25	3.35	1.61
Sr	4.84	1.85	3.48	1.73	3.45	1.69	4.05	1.67	4.84	1.85
Ba	13.31	3.24	7.45	2.37	7.73	2.42	6.75	1.77	13.31	3.24
U			29.54	5.41	28.15	5.09				
Total	100%		100%		100%		100%		100%	

When the size of one crystal is considered to be same as one grain then the physical size is equal to the coherence length. This case is not always valid as one grain can contain ploy crystalline structures. So, it can be considered that the size of crystal is smaller than the size of a grain. The non-uniformity after the doping results in the presence of the large and small grains at higher doping level shown in Fig. 3. The composition x=0.4 shows the platelet formed grains as well there is formation of boundaries which provide the opposition to the applied field which in turn increases the coercivity. With the addition of dopant elements in hexagonal ferrite, complex permittivity ($\varepsilon' - j\varepsilon''$) and complex permeability ($\mu' - j\mu''$) also varies.

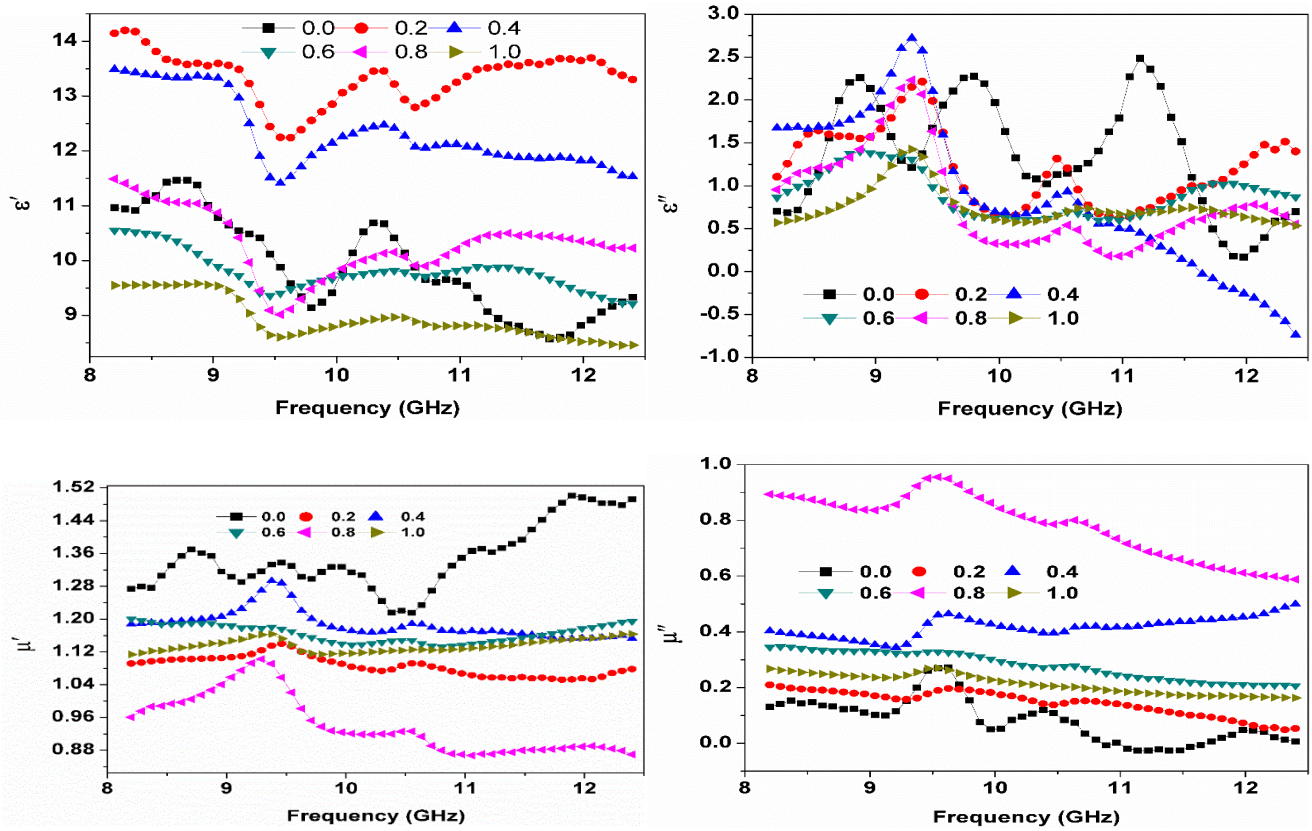

Fig. 4. Variations in complex permittivity, permeability, dielectric and magnetic loss for different samples of $Ba_{0.5}Sr_{0.5}Co_xGa_xFe_{12-2x}O_{19}$ (x = 0.0, 0.2, 0.4, 0.6, 0.8 and 1.0) hexagonal ferrite compositions (color online)

The results shown in Fig. 4 explain these variations according to the composition of Co^{2+}, Ga^{3+} and Fe^{3+} (x=0.0, 0.2, 0.4, 0.6, 0.8 and 1.0). The value of dielectric constant, (ε') is lowest in x=1.0 composition highest with x=0.2. With rest of the compositions, ε' is varying non- linearly. The variations are large at higher frequencies. Whereas dielectric losses(ε'') are maximum at x=0.4. Similarly, complex permeability ($\mu' - j\mu''$) also varies non linearly with the addition of dopants at frequency 8.2GHz-12.4GHz. The variation of reflection loss (Microwave absorption) is better explained by quarter wavelength mechanism. This mechanism shows relation between thickness of composition and wavelength of propagating signal. This relation is explained by the equation given below [19]:

$$t = \frac{n\lambda}{4} = \frac{n.c}{4f\sqrt{\mu_r \varepsilon_r}} \quad (1)$$

where t is thickness of composition, c is velocity of light= $3x10^8$ m/s, $\mu_r = \mu' - j\mu''$, $\varepsilon_r = \varepsilon' - j\varepsilon''$

Fig. 5 explains the variation of reflection loss in M-type $Ba_{0.5}Sr_{0.5}Co_xGa_xFe_{(12-2x)}O_{19}$ (x=0.0,0.2,0.4,0.6,0.8 and 1.0) hexagonal ferrite. It is clear from the results that maximum RL dip of -33.36 dB occurs at x=0.4 composition at 9.62 GHz with 2.0 mm thickness. As discussed above, the relation between RL and thickness of composition is better explained by Quarter wavelength mechanism. The calculated thickness is represented as t_{cal} and thickness at which max RL dip occurs is t_{sim}. The variations of RL dip according to thickness, composition and frequency from the results of graph shown in fig 9-14 is given as: at x=0.0, RL= -23.61dB at 9.62 GHz and x=0.4, RL= -33.36 dB at 9.62 GHz and 2.0mm thickness, 2.2mm thickness, at x=0.2 , RL= -20.08 dB at 9.376 GHz and 2.1mm thickness, at at x=0.6, RL= -25.22dB at 8.95 GHz and 2.4mm thickness, at x=0.8, RL= -14.4dB at 12.4 GHz and 1.8 mm thickness, at x=1.0, RL= -18.12dB at 9.29 GHz and 2.5mm thickness.

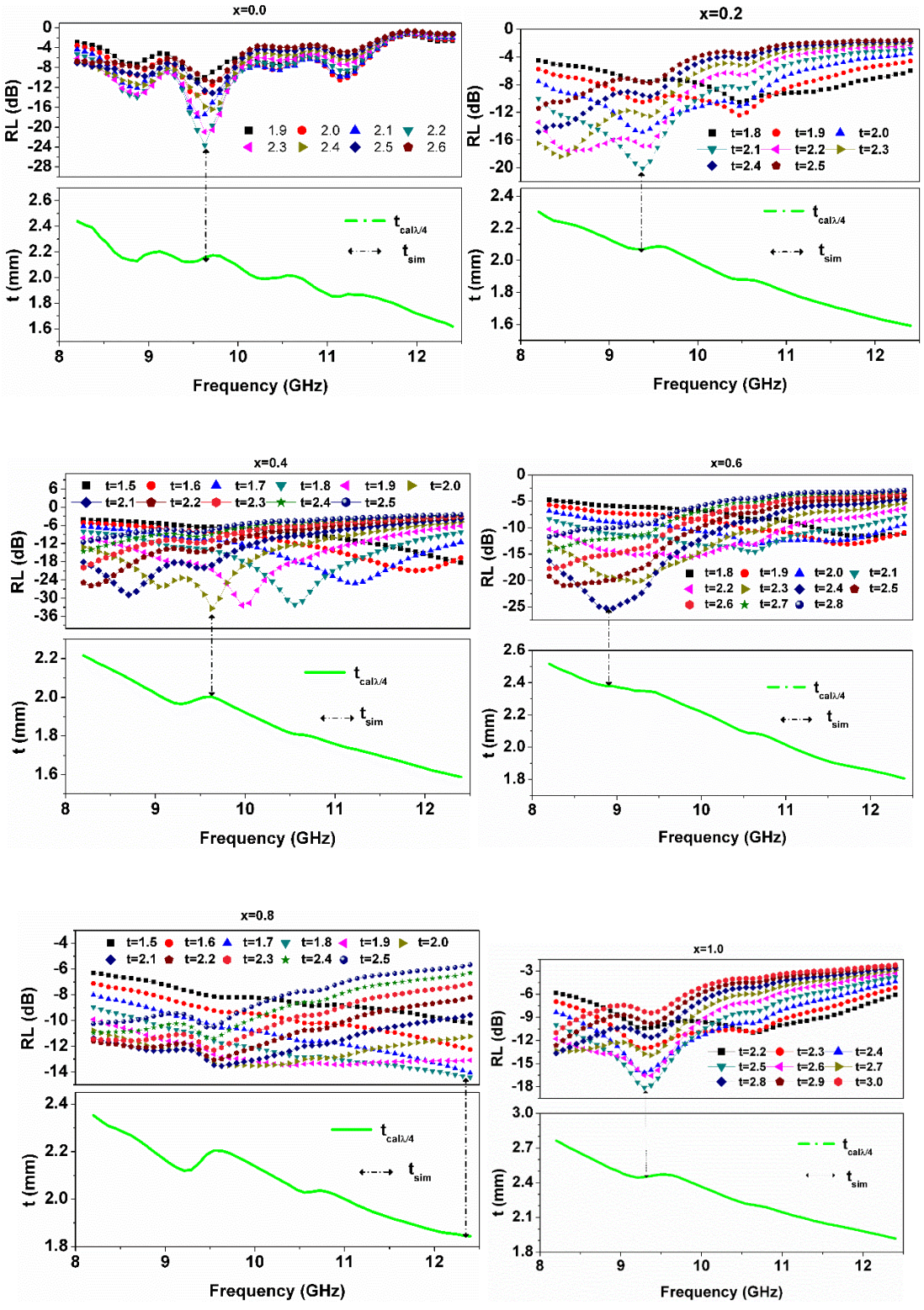

Fig. 5. Variations in reflection loss for different samples of $Ba_{0.5}Sr_{0.5}Co_xGa_xFe_{12-2x}O_{19}$ (x = 0.2, 0.4, 0.6, 0.8 and 1.0) hexagonal ferrite compositions (color online)

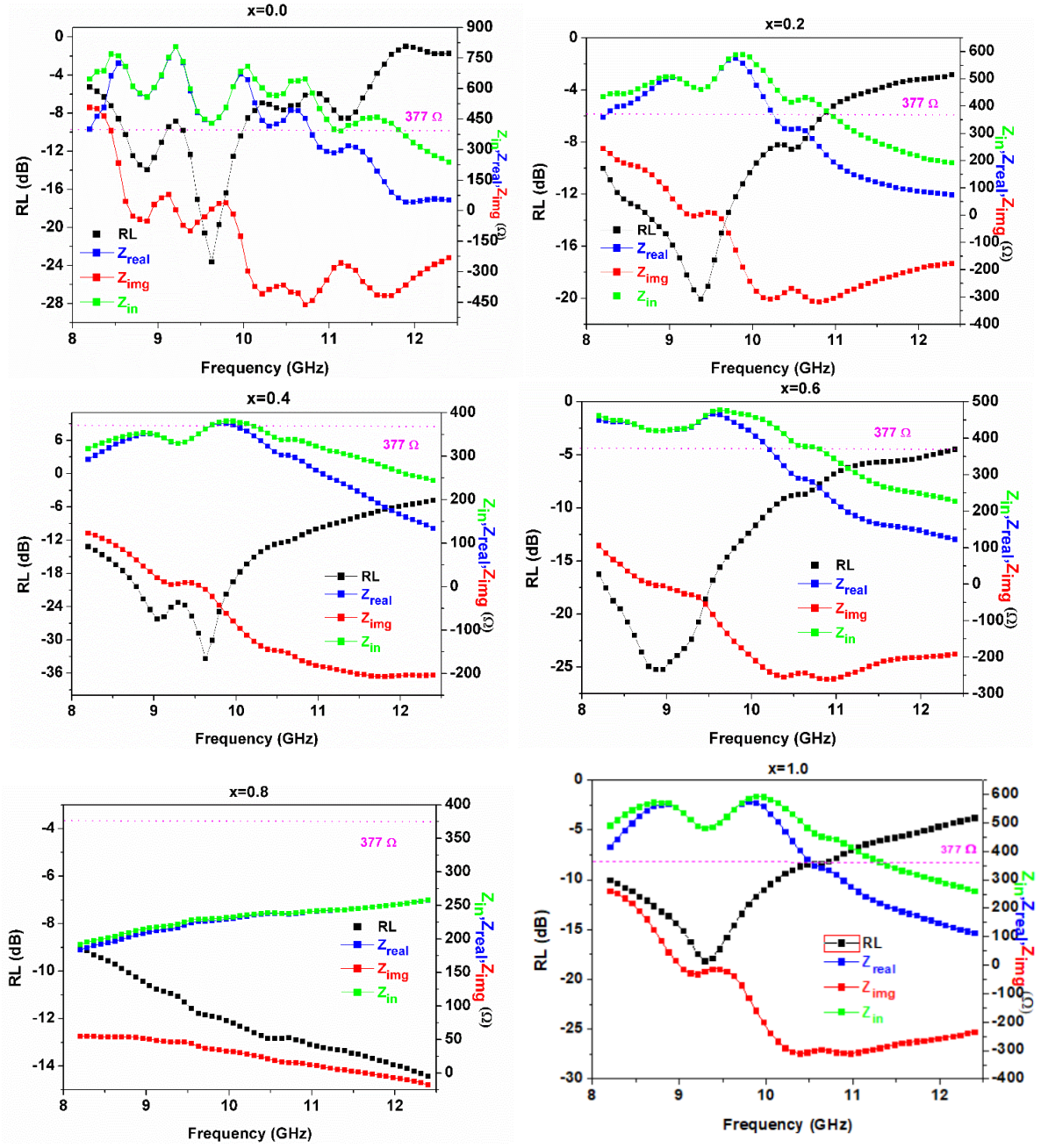

Fig. 6. Variations in reflection loss, Z_{real}, Z_{img}, Z_{in} for different samples of $Ba_{0.5}Sr_{0.5}Co_xGa_xFe_{12-2x}O_{19}$ (x = 0.2, 0.4, 0.6, 0.8 and 1.0) hexagonal ferrite compositions (color online)

The maximum RL dips occurs at x=0.4 and the theoretical results of t_{cal} (2.0mm) match with practical values of t_{sim}(2.002mm). So, here the phenomenon of quarter wavelength is fully satisfied. This is due to the fact that at x=0.4, the dielectric loss (ε'') is maximum i.e., 2.72 at 9.96 GHz. Due to resonance peaks, RL dips of -37.44dB, -34.07dB at 2.0, 2.1mm thickness occurs. This composition also has the lowest coercivity of 17Oe among all compositions. So, all four methods mentioned above i.e. Quarter wavelength, impedance matching and magnetic loss resulted in major RL dip at x=0.4.

According to transmission line theory, RL is also a function of input impedance (Z_{in}). It is expressed below by the equation:

$$RL = 20\log\left|\frac{(z_{in}-z_o)}{(z_{in}+z_o)}\right| \quad (2)$$

Here Z_o is characteristics impedance and its value is standard 377Ω for free space.

Higher the value of RL, higher will be absorption of microwave signal and absorption is maximum when proper impedance matching is there i.e., $z_{in} = z_o$ or $\frac{z_{in}}{z_o} = 1$. The expression for Z_{in} is given below:

$$z_{in} = z_o \sqrt{\frac{\mu_r}{\varepsilon_r}} \tanh\left[j\left(\frac{2\pi f t}{c}\right)\sqrt{\mu_r . \varepsilon_r}\right] \quad (3)$$

Here z_{in} is complex in nature. $z_{in} = z_{real} + z_{img}$ and z_{real} is real impedance & z_{img} is imaginary impedance. From the results shown in Fig. 6, it is clear that when large RL dips occurs when z_{in} is near to z_o i.e., 377Ω. That means real impedance near to 377Ω and imaginary impedance near to zero. At composition x=0.4, maximum RL dip (-33.36dB) occurs. The frequency at this dip is 9.62 GHz and in comparison, to other compositions, z_{in} is close to impedance matching i.e., at this dip, z_{real} is 362.49Ω (near to 377Ω) and z_{img} is -6.44Ω (close to zero). Both these parameters are calculated from the equation of z_{in}. Although z_{real} is 375.48 Ω (closer to 377 Ω) with RL as -21dB at frequency 9.88 GHz and z_{img} is observed to be -61.68Ω (quite away from zero). It is clear that the present situation does not fully satisfy the impedance matching criterion. While describing microwave absorber, bandwidth is also considered as another important parameter. The graphs explains that at composition x=0.8 it can act as wideband absorber (B.W= 4.2GHz) with thickness t=2.0mm & as a narrowband absorber (B.W=0.08 GHz) for composition x=1.0 at thickness t= 3.0 mm , with reflection loss varying from -10 dB to -20 dB and similarly it operates in wideband for composition x=0.4 (BW as 1.1GHz) with thickness of 2mm & as narrowband (BW as 0.42GHz) with reflection loss more than -20 dB.

4. Conclusion

Synthesisation of M-type $Ba_{0.5}Sr_{0.5}Co_xGa_xFe_{(12-2x)}O_{19}$ (x=0.0,0.2,0.4,0.6,0.8 and 1.0) hexagonal ferrite has been successfully completed. Based on analysis using EDAX, SEM and VNA, we have observed that microwave absorption was increasing with the addition of dopants and maximum RL was -33.36 dB with frequency 9.96 GHZ at x=0.4 with 2.0mm thickness. It was also being demonstrated that x=0.8 has wide bandwidth (B. W= 4.2GHz) with thickness as t=2.0mm and act as narrow bandwidth (B. W=0.08 GHz) absorber with increasing thickness to t=3.0mm for composition x=1.0. From the results, it is also clear that microwave absorption also depends upon thickness, input impedance and frequency parameters. So, RL can be tuned corresponding to these parameters. This synthesized microwave absorber can find wide application for absorption of unwanted electromagnetic interference in wireless communication.

Acknowledgements

This work is carried out at G.B Pant Institute of Engineering and Technology, Pauri Garhwal Uttrakhand. We are very grateful to the faculty of Nano Material Sciences & ECE for their valuable support and cooperation. We are also thankful to IKGPTU, Jalandhar for their help and support.

References

[1] S. M. Abbas, R. Chatterjee, A. K. Dixit, A. V. R. Kumar, and T.C. Goel, J. Appl. Phys. **101**, 1 (2007).
[2] R. C. Pullar, Prog. Mater. Sci. **57**, 1191 (2012).
[3] Z. Mosleh, P. Kameli, A. Poorbaferani, M. Ranjbar, H. Salamati, J. Magn. Magn. Mater. **397**, 101 (2016).
[4] A. Baykal, S. Ünver, U. Topal, H. Sözeri, Ceram. Int. **43**, 14023 (2017).
[5] M. M. Syazwan, R. S. Azis, M. Hashim, I. Ismayadi, S. Kanagesan, A. N. Hapishah, J. Aust. Ceram. Soc., **53**, 465 (2017).
[6] L. Deng, Y. Zhao, Z. Xie, Z. Liu, C. Tao, R. Deng, RSC Adv. **8**, 42009 (2018).
[7] Y. E. Gunanto, M. P. Izaak, S. S. Silaban, W. A. Adi, IOP Conf. Ser. Mater. Sci. Eng. **367**, (2018).
[8] İ. Araz, F. Genç, J. Supercond. Nov. Magn. **31**, 279 (2018).
[9] D. Guo, W. Kong, J. Feng, X. Li, X. Fan, J. Alloys Compd. **751**, 80 (2018).
[10] N. Rosdi, R. S. Azis, I. Ismail, N. Mokhtar, M. M. M. Zulkimi, M. S. Mustaffa, Scientific Reports **11,** 15982 (2021).
[11] G. Feng, W. Zhou, H. Deng, D. Chen, Y. Qing, C. Wang, F. Luo, D. Zhu, Z. Huang, Y. Zhou, Ceram. Int. **45**, 13859 (2019).
[12] S. B. Narang, A. Arora, J. Magn. Magn. Mater. **473**, 272 (2019).
[13] İ. Araz, J. Mater. Sci. Mater. Electron. **30**, 5130 (2019).
[14] M. khandani, M. Yousefi, S. S. S. Afghahi, M. M. Amini, M. B. Torbati, Mater. Chem. Phys. **235**, 121722 (2019).
[15] C. Liu, Y. Zhang, Y. Zhang, G. Fang, X. Zhao, K. Peng, J. Zou, J. Alloys Compd. **773**, 730 (2019).
[16] J. Li, S. He, K. Shi, Y. Wu, H. Bai, Y. Hong, W. Wu, Q. Meng, D. Jia, Z. Zhou, Ceram. Int. **44**, 6953 (2018).
[17] Z. Torabi, A. Arab, F. Ghanbari, J. Electron. Mater. **47**, 1259 (2018).
[18] S. Mahadevan, S. B. Narang, P. Sharma, Ceram. Int. **45**, 9000 (2019).
[19] R. M. Almeida, W. Paraguassu, D. S. Pires, R. R. Corrêa, C. W. de Araujo Paschoal, Ceram. Int. **35**, 2443 (2009).

*Corresponding author: kamalbhatia.er@gmail.com